Journal of Nuclear Materials 408 (2011) 25–29

Contents lists available at ScienceDirect

Journal of Nuclear Materials

journal homepage: www.elsevier.com/locate/jnucmat

Electrodeposition of metallic uranium at near ambient conditions from room temperature ionic liquid

Ch. Jagadeeswara Rao, K.A. Venkatesan, K. Nagarajan *, T.G. Srinivasan, P.R. Vasudeva Rao

Fuel Chemistry Division, Indira Gandhi Centre for Atomic Research, Kalpakkam 603 102, India

ARTICLE INFO

Article history:
Received 9 September 2009
Accepted 22 October 2010

ABSTRACT

The electrochemical behavior of U(IV) in the room temperature ionic liquid (RTIL), N-methyl-N-propylpiperidinium bis(trifluoromethylsulfonyl)imide ($MPPiNTf_2$), was investigated to evaluate the feasibility of using the RTIL for non-aqueous reprocessing application. In this context, the rate of dissolution of uranium oxide (UO_2) in $HNTf_2$ was studied at 353 K. The dissolution of UO_2 in $HNTf_2$ was rapid; nearly 50% of UO_2 dissolved within 3 h and more than 95% dissolved in 25 h. The resultant solution was dried, diluted with $MPPiNTf_2$ and the electrochemical behavior of U(IV) in $MPPiNTf_2$ was studied at 373 K at platinum, glassy carbon and stainless steel electrodes. The cyclic voltammograms of U(IV) in $MPPiNTf_2$ at platinum and glassy carbon electrodes consisted of four cathodic waves occurring at a peak potentials of −0.7 V (Fc/Fc^+), −1.4 V, −2.2 V and −2.7 V. Controlled potential electrolysis of a solution of U(IV) in $MPPiNTf_2$ at −2.8 V (Fc/Fc^+) resulted in the deposition of metallic uranium, which was confirmed by X-ray diffraction and scanning electron microscopy.

1. Introduction

Non-aqueous pyrochemical processes [1] are being developed by many countries for reprocessing of spent nuclear fuel, due to the inherent advantages of inorganic salt media such as reduced criticality concern, minimization of liquid waste and ability to handle fuels after shorter cooling times and high burn up. There are two different approaches, namely electrowinning and electrorefining, are available for reprocessing of spent nuclear fuels by pyrochemical means. In the oxide electrowinning process, the actinide oxides are dissolved in alkali or alkaline earth halides as oxychlorides, followed by electrowinning of actinides as oxides. The electrorefining process, which is originally developed for metallic fuels, involves the dissolution of spent nuclear fuel in molten alkali chloride medium followed by selective electrodeposition of actinides. Another process of interest in nuclear industry is the direct electrochemical reduction of actinide oxides [2] to the corresponding metals in molten LiCl or $CaCl_2$ medium, wherein the reduction is assisted by initial deposition of Li or Ca on the actinide oxide. In all these cases, the process temperatures are ~773 K or above depending on the composition of chosen electrolyte.

Room temperature ionic liquids (RTILs) are organic salts molten at temperatures lower than 373 K [3,4]. Generally they are made up of a bulky organic cation and an inorganic or organic anion. For example, substitution of alkali metal ion present in high temperature molten salt by an unsymmetrical organic cation such as 1-butyl-3-methylimidazolium cation ($bmim^+$) results in substantial lowering of melting point of the resultant organic salt, 1-butyl-3-methylimidazolium chloride (bmimCl, m.p. 340 K). Employing such organic salts (or RTILs) in place of inorganic chloride media would lead to the operation of entire process at near ambient conditions [5–8]. Moreover, the cation and anion combination of RTIL can be manipulated in such a way to enhance the solubility of actinides as well as to obtain a completely incinerable electrolyte, which is indeed desirable for the disposal of spent electrolyte.

In this context, Nikitenko et al. [9–11] investigated the spectroscopic and electrochemical aspects of U(IV)-hexachloro complexes in 1-butyl-3-methylimidazolium bis(trifluoromethylsulfonyl)imide ($bmimNTf_2$), tri-*n*-butylmethylammonium bis(trifluoromethylsulfonyl)imide ($[Mebu_3N][NTf_2]$) hydrophobic ionic liquids. Based on the observation of a cathodic wave at −3.2 V (vs. Ag/AgCl) in the cyclic voltammogram of $[UCl_6]^{2-}$ in $[Mebu_3N][NTf_2]$, Nikitenko et al. suggested that the reduction of U(III) to U(0) occurred at −3.0 V. They also investigated the coordination behavior of Np(IV) and Pu(IV) in $bmimNTf_2$. Bhatt et al. [12–14] studied the electrochemistry of some lanthanides, La^{3+}, Sm^{3+} and Eu^{3+} in $[R_4X][NTf_2]$, where X = N, P and As. Since the RTIL, $[Me_4X][NTf_2]$, has a extremely large electrochemical window (>5 V), they proposed to use it as electrolytic medium for electrodeposition of uranium and plutonium. In addition, they also studied the reduction of La^{3+}, Sm^{3+} and Eu^{3+} to metallic state in the RTIL, $[Me_3NBu][NTf_2]$, and reported similar results as in the previous case [13]. The voltammetric behavior of $[Th(NTf_2)_4(HNTf_2)]\cdot 2H_2O$ was also studied [14] in $[Me_3NBu][NTf_2]$. Th(IV) in this ionic liquid was reduced to Th(0) by a single

* Corresponding author. Fax: +91 44 27480065.
E-mail address: knag@igcar.gov.in (K. Nagarajan).

0022-3115/$ - see front matter © 2010 Elsevier B.V. All rights reserved.
doi:10.1016/j.jnucmat.2010.10.022

reduction step. However, due to the presence of moisture in the ionic liquid, the product Th(0) was converted to ThO_2 during reduction. Legeai et al. [15] reported the electrodeposition of lanthanum from 1-octyl-1-methylpyrrolidinium bis(trifluoromethylsulfonyl)imide ionic liquid.

We have earlier reported [5,6] the electrochemical behavior of U(VI) in 1-butyl-3-methylimidazolium chloride (bmimCl) and Eu(III) in N-butyl-N-methylpyrrolidinium bis(trifluoromethylsulfonyl)imide ($BMPyNTf_2$). U(VI) in bmimCl undergoes a single step two-electron transfer reduction to uranium oxide deposit at glassy carbon working electrode, and Eu(III) to metallic europium at stainless steel electrode. In this paper, we report the results of the studies on the electrochemical behavior of U(IV) in a room temperature ionic liquid, N-methyl-N-propylpiperidinium bis(trifluoromethylsulfonyl)imide ($MPPiNTf_2$), to evaluate the feasibility of using $MPPiNTf_2$ for the electrodeposition of uranium. Unlike the direct oxide reduction of actinide oxide as discussed above, the present study deals with the dissolution of UO_2 in $HNTf_2$ followed by electrodeposition of actinides in metallic form from $MPPiNTf_2$. The results of the studies on the rate of dissolution of UO_2 in $HNTf_2$, the electrochemical behavior of U(IV) in $MPPiNTf_2$ using cyclic voltammetry at various electrodes, and the surface morphology of the deposit are discussed in this paper.

2. Experimental

2.1. Materials

All the chemicals used in this study were of analytical reagent grade. N-methylpiperidine, bistrifluoromethylsulfonimide and lithium bis(trifluoromethylsulfonyl)imide were procured from M/s. Fluka, and 1-bromopropane from M/s. Lancaster. The method for the preparation of $MPPiNTf_2$ is described elsewhere [16]. UO_2 was obtained by reducing UO_3 by heating the UO_3 powder at 1073 K under 8% H_2/Ar (pre-equilibrated in water at 273 K) for 20 h. The average particle size of UO_2 thus obtained was determined to be 20 μm.

2.2. Dissolution of UO_2 in $HNTf_2$

The rate of dissolution of UO_2 in $HNTf_2$ solution was studied by refluxing (~373 K) a mixture of UO_2 powder (0.48 g, av. particle size 20 μm) and $HNTf_2$ (2 g), which were taken in 1:4 (U:$HNTf_2$) mole ratio in water (30 mL) medium. The solution was taken in a 100 mL round bottomed flask equipped with a condenser was immersed in a oil bath for maintaining constant temperature and the solution was stirred using magnetic stirring bar (1 cm dia.). A known volume of aliquot was drawn from the supernatant at various intervals of time for analyzing uranium present in the solution by spectrophotometric method using Arsenazo III as colouring agent. After complete dissolution of UO_2, the water present in aqueous phase was removed by rotary evaporator, and the dry solid was added to $MPPiNTf_2$ for electrochemical studies.

2.3. Voltammetric studies

The concentration of U(IV) in $MPPiNTf_2$ was kept at ~80 mM. Voltammetric studies were carried out at 373 K. A glassy carbon rod (cylindrical SA = 0.47 cm^2), a SS rod (cylindrical SA = 0.27 cm^2) or Pt wire (cylindrical SA = 0.11 cm^2) were used as working electrodes. Glassy carbon rod and Pd wire acted as counter and quasi-reference electrodes respectively. The internal standard Fc/Fc^+ was added to $MPPiNTf_2$ and all the redox potentials were measured against the Fc/Fc^+ redox couple. The electrochemical cell had a single leak-tight compartment and all the electrodes were placed in the same compartment. The cell was kept under argon atmosphere during entire study. Electrodeposition studies were carried out on either SS (SA = 16 cm^2) or platinum (SA = 2 cm^2) electrode and Pt counter electrode (SA = 2 cm^2). Faradaic efficiency was calculated from the ratio of uranium actually deposited to the uranium metal deposit expected for the quantity of coulombs passed into the solution.

2.4. Instrumentation

Cyclic voltammograms of the solutions were recorded using Autolab 302 N (PGSTAT-030) equipped with an IF 030 interface. Micro-elemental CHNS analysis was carried out using Elementer Vario-EL. X-ray diffraction pattern of uranium deposit was obtained using Philips 1011 X-ray diffractometer (operating with 40 kV and 45 mA) with Cu Kα (1.5406 Å) radiation. UV–VIS absorption spectrum was determined using Shimadzu UV–VIS–NIR spectrophotometer model UV-3600. A Philips field effect (model XL 30) scanning electron microscope (SEM) with energy-dispersive spectrometer (EDS) working at 30 kV was used to examine the surface morphology and elemental composition of the deposit. The particle size of UO_2 was determined by using Malvern Master sizer, Model microplus v 2.15, particle size analyzer.

3. Results and discussion

3.1. Dissolution of UO_2

Dissolution of UO_2 in $HNTf_2$ solution, as a function of time, is shown in Fig. 1. It is observed that uranium dissolution increases with increase of time. Nearly 50% of UO_2 dissolved within 3 h and more than 95% in 25 h. The dissolution reaction is shown in Eq. (1). The green colour solution obtained was evaporated for several hours at 343 K to remove water and the dry solid was added to $MPPiNTf_2$ to get a ~80 mM solution for voltammetric studies. The micro-elemental analysis of the uranium complex yielded (theoretical value in parenthesis) C 6.89 (7.07), H 0.28 (0), N 4.01 (4.12), S 18.2 (18.85), U 17.3 (17.5), indicates the composition of the complex could be $U(NTf_2)_4$ (H_2O is insignificant).

$$UO_2 + 4HNTf_2 \xrightarrow{\text{reflux, stir}} U(NTf_2)_4 + 2H_2O \quad (1)$$

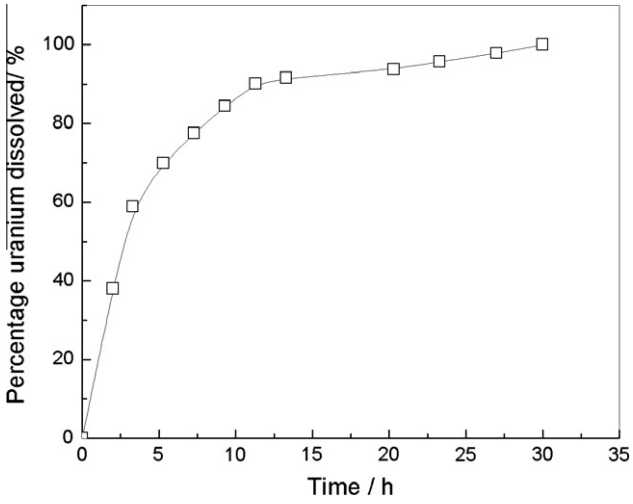

Fig. 1. Dissolution of UO_2 in $HNTf_2$ as a function of time at 353 K. U:$HNTf_2$ 1:4 mol ratio.

3.2. Cyclic voltammetry

The cyclic voltammograms of a solution of U(IV) in $MPPiNTf_2$ recorded at a scan rate of 10 mV/s at platinum, glassy carbon and stainless steel electrodes are shown in Fig. 2. The voltammograms recorded at platinum and glassy carbon are quite similar, whereas few cathodic waves are merged when recorded at stainless steel electrode. Fig. 3 shows the cyclic voltammogram of U(IV) in $MPPiNTf_2$ recorded at platinum electrode at a scan rate of 10 mV/s at various switching potentials. The reduction wave (E_p^{c1}) occurring at a peak potential of −0.76 V (vs. Fc/Fc^+) could be attributed to the reduction of U(IV). This reduction results in a couple of oxidation waves, a weaker one (E_p^{a1}) occurring at −0.52 V (vs. Fc/Fc^+) and a stronger (E_p^{a2}) occurs at 0.05 V (vs. Fc/Fc^+), when switched at −1.0 V (vs. Fc/Fc^+). The intensities of these oxidation waves increase, when the voltammogram is switched after the second reduction wave (E_p^{c2}), which occurs at −1.14 V (vs. Fc/Fc^+). However, (E_p^{c2}) is not accompanied by any additional oxidation wave upon scan reversal. This shows that (E_p^{c2}) may be irreversible or the reduction waves, E_p^{c1} and E_p^{c2}, correspond to the reduction of U(IV) only, perhaps existing in different complex forms. Shirasaki et al. [17] reported a similar behavior for $U(ClO_4)_4(DMSO)_8$

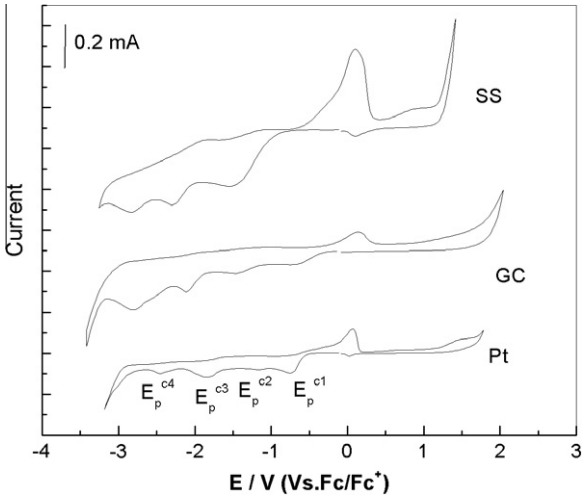

Fig. 2. Cyclic voltammograms of U(IV) in $MPPiNTf_2$ at platinum, glassy carbon and stainless steel electrodes. Temperature: 373 K.

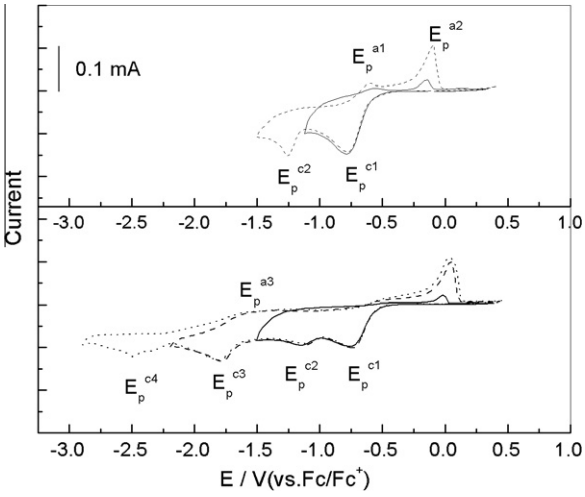

Fig. 3. Cyclic voltammograms of U(IV) in $MPPiNTf_2$ at Pt electrode at different switching potentials. Temperature: 373 K.

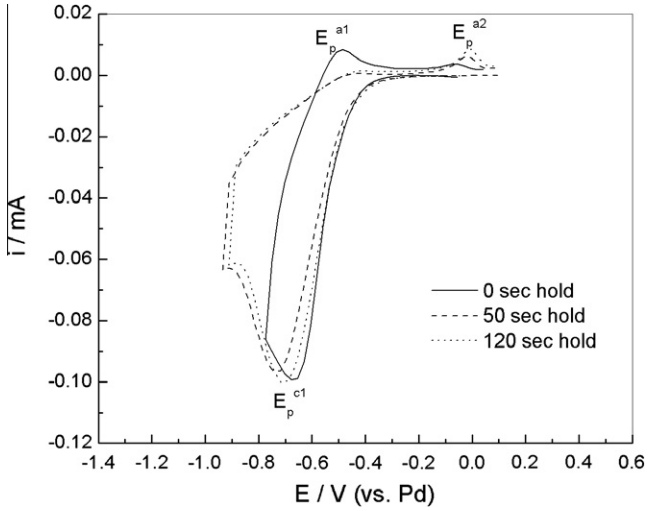

Fig. 4. Cyclic voltammograms of U(IV) in $MPPiNTf_2$ at Pt electrode at different duration of hold at switching potential.

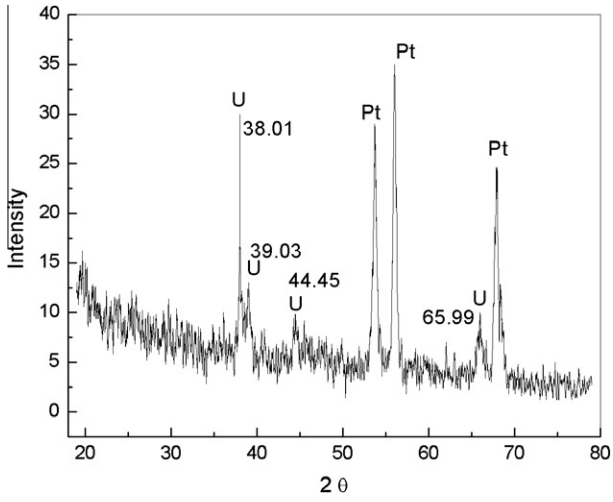

Fig. 5. XRD of uranium metal deposited from $MPPiNTf_2$ on Pt electrode.

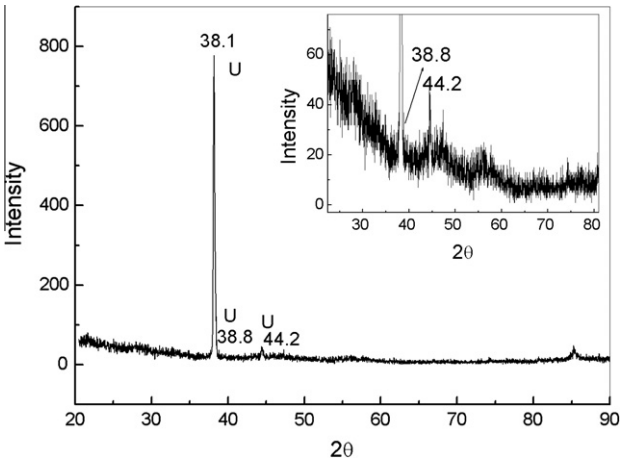

Fig. 6. XRD of uranium metal deposited from $MPPiNTf_2$ on stainless steel electrode.

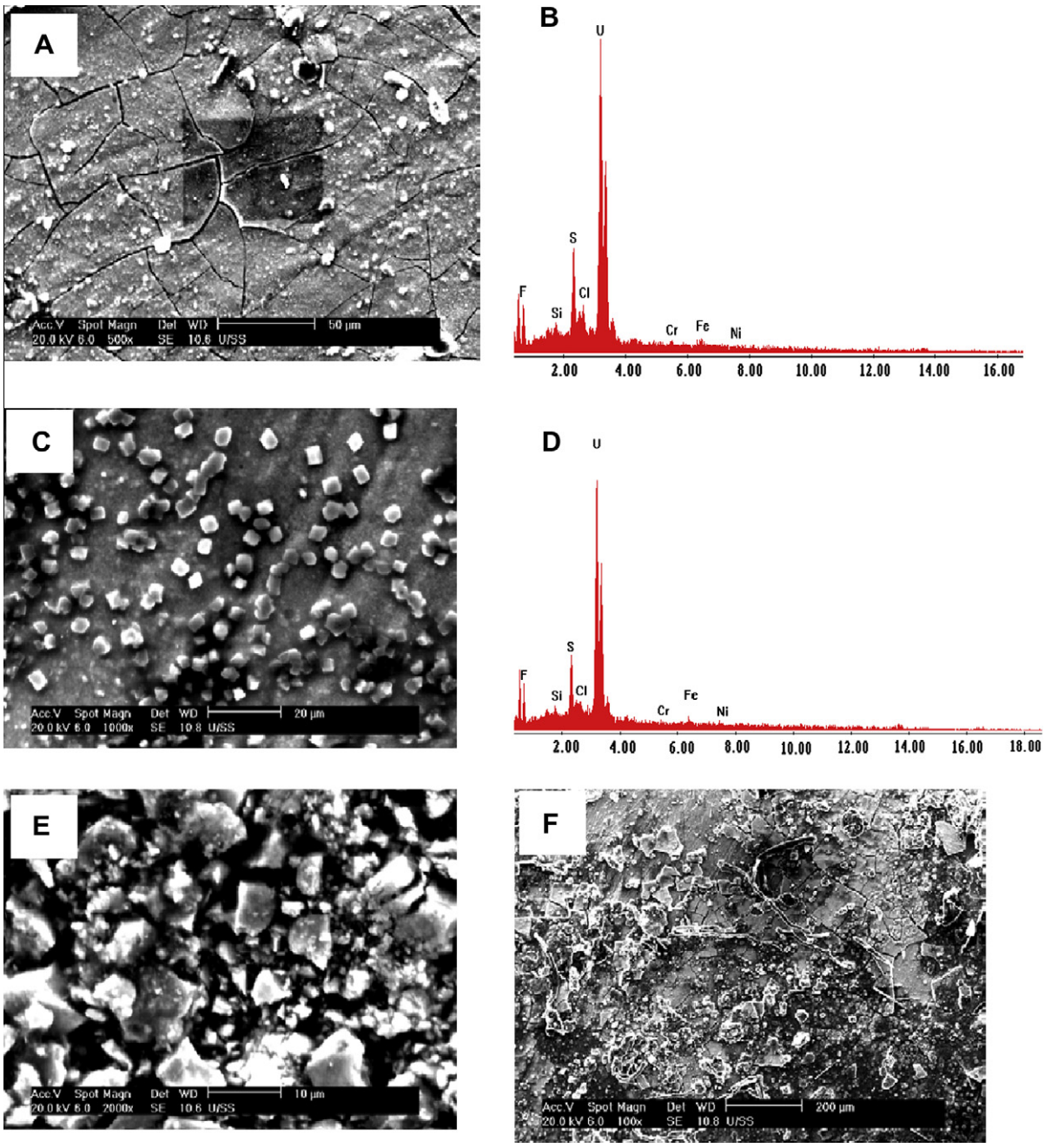

Fig. 7. SEM images and EDS analysis of metallic uranium deposit on stainless steel electrode. (A) Magnification = 500×, (B) EDS analysis of image A, (C) magnification = 1000×, (D) EDS analysis of cube shaped part of image C, (E) magnification = 2000×, (F) magnification = 100×.

complexes at platinum electrode. Based on observations similar to the ones given above, Shirasaki et al. argued that the first three reduction waves obtained at platinum working electrode were due to the reduction of U(IV) to U(III) only. Fig. 4 shows the cyclic voltammograms of U(IV) in $MPPiNTf_2$ recorded at platinum electrode with a hold at the cathodic switching potential of −1.0 V (vs. Fc/Fc^+), for a specific duration. It is observed that the anodic currents are fairly similar irrespective of the duration of hold. The increase of anodic current, expected from this cathodic hold, is not observed in the present case. However, significant increase in anodic current is observed only, when the cathodic scan is switched after the second reduction wave, E_p^{c2} as shown in Fig. 3. All these observations indicate that the reduction waves, E_p^{c1} and E_p^{c2} may perhaps belong to the reduction of U(IV), which are existing in different complex forms, to U(III), which is in agreement with work of Shirasaki et al. [17].

The cyclic voltammogram of U(IV) shown in Fig. 3 also consists of two more reduction waves occurring at peak potentials, E_p^{c3} and E_p^{c4}, of −1.8 V (vs. Fc/Fc^+) and −2.5 V (vs. Fc/Fc^+) respectively. The reduction wave E_p^{c3} is accompanied by a less intense oxidation wave, E_p^{a3} , and E_p^{c4} is irreversible. Controlled potential electrolysis of U(IV) in $MPPiNTf_2$ at platinum electrode (2 cm^2) at −1.9 V (vs. Fc/Fc^+) does not result in any deposition. However, when carried out at −2.4 V (vs. Fc/Fc^+), the electrode was coated with a thick black deposit. The XRD pattern of the deposit, shown in Fig. 5, matches the pattern reported for uranium metal (JCPDS No. 06-0553) confirms the deposition of uranium on platinum electrode.

The Faradaic efficiency was determined to be ~80%. This shows that the cathodic wave E_p^{c4} is responsible for the reduction of uranium into metallic form. The electrochemical behavior of U(IV) in $MPPiNTf_2$ at glassy carbon electrode is very similar to the behavior observed at platinum electrode.

Based on these results electrochemical behavior and electrodeposition of uranium in bulk was studied at stainless steel working electrode, due to its easy availability and inexpensiveness. The electrochemical behavior of U(IV) in $MPPiNTf_2$ at stainless steel electrode (SA = 0.27 cm^2) is marginally different from that at platinum and glassy carbon electrodes. The cyclic voltammogram of U(IV) in $MPPiNTf_2$ at stainless steel electrode is shown in Fig. 2. The cathodic waves E_p^{c1} and E_p^{c2} observed at other electrodes, due to the reduction of U(IV) to U(III), have merged together at −1.55 V (Fc/Fc^+) in the present case. The voltammogram also consists of other cathodic waves occurring at −2.3 V and −2.8 V. Controlled potential electrolysis of U(IV) in $MPPiNTf_2$ at stainless steel plate electrode (16 cm^2) at −2.3 V (vs. Fc/Fc^+) does not result in any deposition. However, electrolysis at −2.8 V (vs. Fc/Fc^+), results in a deposition of uranium in metallic form. The XRD pattern of the deposit is shown in Fig. 6, whose 100% intensity peak is in agreement with that of the standard pattern of metallic uranium (JCPDS No. 06-0553). The other peaks are also seen in the pattern albeit with less intensity as shown in Fig. 6 inset. Nevertheless, it is important to note that the deposit do not exhibit the XRD-pattern of any uranium oxide. The SEM image of the deposit is shown in Fig. 7. It is observed that the deposit is uniform all over the surface (Fig. 7A), and in several places cube shaped nuclei (Fig. 7C and E at higher magnification) are seen. Fig. 7F shows the SEM micrograph of the deposit obtained at different place at lower magnification (100×). EDS analysis of the deposit at various places, shown in Fig. 7B for uniform surface and Fig. 7D for cube shaped nuclei, indicates the presence of uranium both at crystallized surface and other places. The Faradaic efficiency of the process was about 80%.

4. Conclusions

The ionic liquid, $MPPiNTf_2$, offers wide electrochemical window and extended cathodic stability suitable for the electrodeposition of lanthanides and actinides in metallic form. Uranium oxide and perhaps other oxides of lanthanides and actinides can be conveniently dissolved by treating with $HNTf_2$ followed by electrodeposition from $MPPiNTf_2$. However, more studies such as radiation stability of $MPPiNTf_2$, electrochemical behavior of other actinides like plutonium and the effect of other fission products are needed for establishing the potential uses of ionic liquids for non-aqueous reprocessing applications.

Acknowledgements

The authors thank G. Paneerselvam and R. Sudha, Chemistry Group, IGCAR for providing XRD pattern and SEM images respectively.

References

[1] C.C. Mcpheeters, R.D. Pierce, T.P. Mulcahey, Prog. Nucl. Energy 31 (1997) 175–186.
[2] C.S. Seo, S.B. Park, B.H. Park, K.J. Jung, S.W. Park, S.H. Kim, J. Nucl. Sci. Technol. 43 (2006) 587–595.
[3] T. Welton, Chem. Rev. 99 (1999) 2071–2084.
[4] M.J. Earle, K.R. Seddon, Pure Appl. Chem. 72 (2000) 1391–1398.
[5] P. Giridhar, K.A. Venkatesan, T.G. Srinivasan, P.R. Vasudeva Rao, Electrochim. Acta 52 (2007) 3006–3012.
[6] Ch. Jagadeeswara Rao, K.A. Venkatesan, K. Nagarajan, T.G. Srinivasan, P.R. Vasudeva Rao, Electrochim. Acta 54 (2009) 4718–4725.
[7] P. Giridhar, K.A. Venkatesan, S. Subramaniam, T.G. Srinivasan, P.R. Vasudeva Rao, Radiochim. Acta 94 (2006) 415–420.
[8] A.P. Abbott, K.J. McKenzie, Phys. Chem. Chem. Phys. 8 (2006) 4265–4279.
[9] S.I. Nikitenko, C. Cannes, Inorg. Chem. 44 (25) (2005) 9497–9505.
[10] S.I. Nikitenko, C. Hennig, M.S. Grigoriev, C.L. Naour, C. Cannes, D. Trubert, E. Bossé, C. Berthon, P. Moisy, Polyhedron 26 (2007) 3136–3142.
[11] S.I. Nikitenko, P. Moisy, Inorg. Chem. 45 (3) (2006) 1235–1242.
[12] A.I. Bhatt, I. May, V.A. Volkovich, M.E. Hetherington, B. Lewin, R.C. Thied, N. Ertok, J. Chem. Soc. Dalton Trans. (2002) 4532–4534.
[13] A.I. Bhatt, I. May, V.A. Volkovich, D. Collison, M. Helliwell, I.B. Polovov, R.G. Lewin, Inorg. Chem. 44 (2005) 4934–4940.
[14] A.I. Bhatt, N.W. Duffy, D. Collison, I. May, R.G. Lewin, Inorg. Chem. 45 (2006) 1677–1682.
[15] S. Legeai, S. Diliberto, N. Stein, C. Boulanger, J. Estager, N. Papaiconomou, M. Draye, J.D. Holbrey, Electrochem. Commun. 10 (2008) 1661–1664.
[16] H. Sakaebe, H. Matsumoto, Electrochem. Commun. 5 (2003) 594–598.
[17] K. Shirasaki, T. Yamamura, T. Herai, Y. Shiokawa, J. Alloys Compd. 418 (2006) 217–221.